Design and control of acetylcholine receptor conformational change

Snehal V. Jadey[a], Prasad Purohit[a], Iva Bruhova[a], Timothy M. Gregg[b], and Anthony Auerbach[a,1]

[a]Department of Physiology and Biophysics, 309 Cary Hall, State University of New York, Buffalo, NY 14214; and [b]Department of Chemistry and Biochemistry, Canisius College, Buffalo, NY 14208

Edited by Jean-Pierre Changeux, Institut Pasteur, Paris Cedex 15, France, and approved January 26, 2011 (received for review November 8, 2010)

Allosteric proteins use energy derived from ligand binding to promote a global change in conformation. The "gating" equilibrium constant of acetylcholine receptor-channels (AChRs) is influenced by ligands, mutations, and membrane voltage. We engineered AChRs to have specific values of this constant by combining these perturbations, and then calculated the corresponding values for a reference condition. AChRs were designed to have specific rate and equilibrium constants simply by adding multiple, energetically independent mutations with known effects on gating. Mutations and depolarization (to remove channel block) changed the diliganded gating equilibrium constant only by changing the unliganded gating equilibrium constant (E_0) and did not alter the energy from ligand binding. All of the tested perturbations were approximately energetically independent. We conclude that naturally occurring mutations mainly adjust E_0 and cause human disease because they generate AChRs that have physiologically inappropriate values of this constant. The results suggest that the energy associated with a structural change of a side chain in the gating isomerization is dissipated locally and is mainly independent of rigid body or normal mode motions of the protein. Gating rate and equilibrium constants are estimated for seven different AChR agonists using a stepwise engineering approach.

ion channel | nicotinic | allosteric | protein engineering

Structure and energy together define the mechanism of protein conformational change. The energy changes that occur when a protein changes shape are manifest in the rate and equilibrium constants of the process. Here, we describe a method of engineering the conformational change of an allosteric protein so that these constants can be measured easily, accurately, and precisely.

Nicotinic acetylcholine receptor-channels (AChRs) are membrane proteins that spontaneously isomerize ("gate") between a resting, closed-channel conformation (R) and an active, open-channel conformation (R*) (1–4). Each of these five-subunit synaptic receptors has two ligand binding sites in the extracellular domain. The $R \leftrightarrow R^*$ gating equilibrium constant is influenced by the presence of small molecules at these sites. When devoid of ligands, neuromuscular AChRs almost always adopt the resting-closed shape, but when both sites are occupied by the neurotransmitter acetylcholine (ACh) they usually are, transiently, active-open. The driving force for the increase in the gating equilibrium constant with ACh at the binding sites is the higher affinity for the transmitter molecules in R* compared to R (5–7).

The most accurate way to measure AChR gating rate and equilibrium constants is by using single-channel, patch-clamp electrophysiology. This method allows the separation of gating events from those associated with other reactions such as ligand binding and desensitization, and at an approximately 10 μs, single-molecule resolution. Typically, the diliganded gating equilibrium constant (E_2) is measured in the presence of agonist molecules. This constant is the product of the unliganded gating equilibrium constant (E_0) and the square of the ratio of equilibrium dissociation constants in R vs. R* (Fig. S1). λ quantifies the extent to which the gating equilibrium constant increases with each additional agonist molecule.

Different agonists promote the channel-opening gating conformational change to different extents because they experience different degrees of affinity increase when the protein adopts R*. Mutations, however, can change E_2 by changing E_0, λ or both. Mutations of some residues that are not close to the transmitter binding sites have been shown to change E_2 only by changing E_0 (8), whereas mutations of some residues that are immediately at the transmitter binding sites have been shown to change both E_0 and λ, sometimes in opposite ways (9, 10).

To understand the molecular determinants of agonist efficacy and the mechanism of the AChR conformational change it is useful to quantify λ and E_0 values for many different ligand-receptor combinations. This information guides our understanding of the energy changes that occur at the binding sites and throughout the AChR when this protein changes shape. However, some ligand-receptor combinations result in AChRs that have gating rate and equilibrium constants that cannot be measured experimentally because they are too large or small. Such combinations include extremely low- or high-efficacy agonists or AChRs with mutations that decrease or increase gating substantially. Also, some mutations reduce the affinity of the binding sites to such an extent that it is not possible to detect ligand-activated currents because high concentrations of agonists can block ion flow through the channel.

We have employed a protein engineering approach that circumvents the problems associated with the bandwidth limitations of single-channel electrophysiology. We change the experimental conditions and tailor the AChR itself by making mutations so that the emergent rate and equilibrium constants are within an optimal window for single-channel analysis. Then, with quantitative knowledge of the effect of the background perturbation(s), we calculate the constants for a reference condition. We estimate λ values for seven different agonists, including several that have never before been examined at the single-channel level. We also apply the method to two AChR mutants and estimate equilibrium dissociation constants for several agonists.

Results

Calibration and Removal of Channel Block. Our first objective was to estimate the diliganded forward and backward gating rate constants (f_2 and b_2) and equilibrium constant ($E_2 = f_2/b_2$) under a reference condition: wild-type $\alpha_2\beta\delta\epsilon$ AChRs expressed in HEK cells, PBS in the bath, pipette potential +70 (membrane potential approximately −100 mV), 23 °C. We chose agonists that elicit currents that have interval lifetimes that are in a suitable range for single-channel analysis. The three agonists we studied were dimethyl pyrrolidinium (DMP), dimethyl thiazolidinium (DMT), and dimethyl thiomorpholinium (DMThM) (Fig. 1). The rate and equilibrium constant estimates from these experi-

Author contributions: S.V.J., P.P., and A.A. designed research; S.V.J., P.P., and I.B. performed research; T.M.G. contributed new reagents/analytic tools; and A.A. wrote the paper.

The authors declare no conflict of interest.

This article is a PNAS Direct Submission.

[1]To whom correspondence should be addressed. E-mail: auerbach@buffalo.edu.

This article contains supporting information online at www.pnas.org/lookup/suppl/doi:10.1073/pnas.1016617108/-/DCSupplemental.

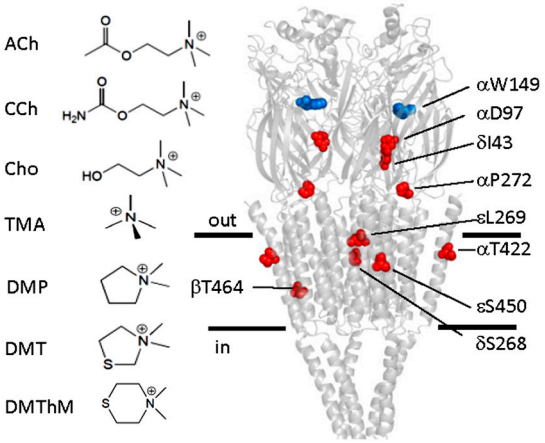

Fig. 1. (*Left*) Agonists (full name given in *SI Text*). (*Right*) Torpedo AChR (accession number 2bg9.pdb). Transmitter binding site residues αW149 are blue and mutated residues are red. The mutated amino acids are scattered throughout the protein but are not at the transmitter binding sites. Another view and separate background constructs are shown in Fig. S2.

ments will be used to calibrate other ligand-receptor combinations that are more difficult to quantify under the reference condition.

At 1 mM DMP, channel openings occurred in clusters where each represented the activity of a single AChR (Fig. 2*A*). We limited our analyses only to open and shut intervals within clusters. The open-channel lifetime was well described by a single exponential, and at this agonist concentration, its inverse is a good approximation for b_2 (Fig. 2*C*). The interpretation of the shut, intracluster interval durations is more complex. When the two binding sites are not fully occupied by agonists the main shut component depends on both agonist-binding and channel-gating processes and, therefore, does not reflect just f_2. To separate binding

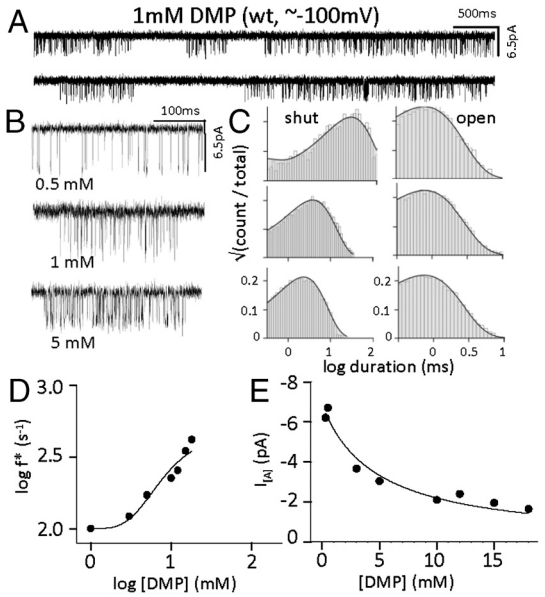

Fig. 2. Gating of AChRs activated by DMP (reference conditions: WT $\alpha_2\beta\delta\epsilon$, approximately −100 mV, 23 °C). (*A*) Clusters of openings that each reflects binding and gating activity of an individual AChR (open is down). (*B*) Higher resolution view of clusters at different [DMP]. (*C*) Intracluster interval duration histograms at different [DMP]. The solid lines are the global fit across concentrations (Scheme S1; K_d = 1.9 mM) with the gating rate constants of the B1 background (Fig. 3*C*). (*D*) Effective opening rate (f*) as a function of [DMP]. Solid line is the Hill equation using the opening rate constant of the B1 background (Fig. 3*D*). (*E*) At this membrane voltage the single-channel current amplitude ($I_{|A|}$) decreases with increasing [DMP] because of fast channel block by agonist molecules.

and gating we increased the agonist concentration in an attempt to saturate the binding sites and isolate just the gating step. As the binding sites are increasingly filled the inverse duration of the main shut component will reach an asymptote at f_2. Fig. 2*D* shows that the effective opening rate increased with increasing [DMP], but that even at the highest concentration tested (12 mM) it had not reached a plateau.

It was not possible to increase the agonist concentration further because of fast channel block by the agonist. DMP resides in the pore only briefly so the gaps in the open intervals arising from block are not resolved as discrete events by our instrument. Rather, these events can be inferred because they decrease the apparent single-channel current amplitude. The equilibrium dissociation constant for block (K_B) can be estimated approximately from dependence of the current amplitude on the agonist (blocker) concentration (Eq. S3). Fig. 2*E* shows that the single-channel current amplitude decreased as a function of [DMP], with $K_B \approx$ 4.7 mM for DMP under the reference condition. As a rule of thumb, and specifically for the AChR, it is possible to both saturate the binding sites and avoid excessive channel block only when the ratio $K_B/K_d > \sim 3$, where K_d is the equilibrium dissociation constant of the R conformation transmitter binding site. This ratio for DMP, unfortunately, is less than this threshold.

Membrane depolarization reduces channel block. DMP is positively charged and the site of channel block is within the electric field of the membrane, so K_B will increase as the membrane is depolarized (11). For other similarly charged blockers of AChRs, K_B increases e-fold with approximately 50 mV depolarization (12). We expected that changing the membrane potential to +100 mV would increase K_B by about 50-fold and allow us to use higher concentrations of DMP in our attempt to saturate the transmitter binding sites. Note that in our experiments we did not need to know the exact extent to which depolarization relieves channel block.

Membrane depolarization also alters the gating rate and equilibrium constants, mainly by increasing b_2. That is, depolarization is a low-Φ, loss-of function perturbation (Eq. S2) (13). This change in the gating rate constants is undesirable because b_2 could approach the upper limit of the patch clamp resolution.

To compensate for the effect of voltage we added a background mutation. The ϵ subunit residue S450 is in the M4 segment of the transmembrane domain and is far from both the transmitter binding sites and the lumen of the channel (Fig. 1 and Tables S1 and S2). Most mutations here have approximately equal-but-opposite effects on gating as does depolarization (are low-Φ, gain-of-function) (14). We found that with DMP, open interval lifetime durations of εS450W AChRs at +100 mV were approximately the same as for WT AChRs at the reference condition (0.58 ± 0.08 vs. 0.55 ± 0.05 ms; mean ± s.d., 10 patches) (see also Fig. 3*C*). We conclude that this M4 mutation in combination with depolarization to +100 mV results in AChRs having the same gating kinetics as those in the reference condition, but with outward currents and greatly reduced channel block. We will refer to this doubly perturbed experimental background as B1 (Table S3 and Fig. S2). Note the fact that the εS450W and depolarization perturbations cancel almost exactly is a convenience, not a necessity. We could have used other mutant/voltage combinations to reduce block, in which case the gating rate constants under the reference condition could be calculated by multiplying the perturbed rate constants by the appropriate fold-changes for that particular combination.

By using B1 we could now study higher concentrations of DMP and fully saturate the transmitter binding sites without contamination from channel block. Fig. 3*D* shows that the effective opening rate increases with [DMP] >12 mM, but was constant between 30–140 mM. This indicates that at these high DMP concentrations binding site saturation had been achieved. The (outward) single-channel current amplitude did decrease slightly between 100 and 140 mM because channel block was not comple-

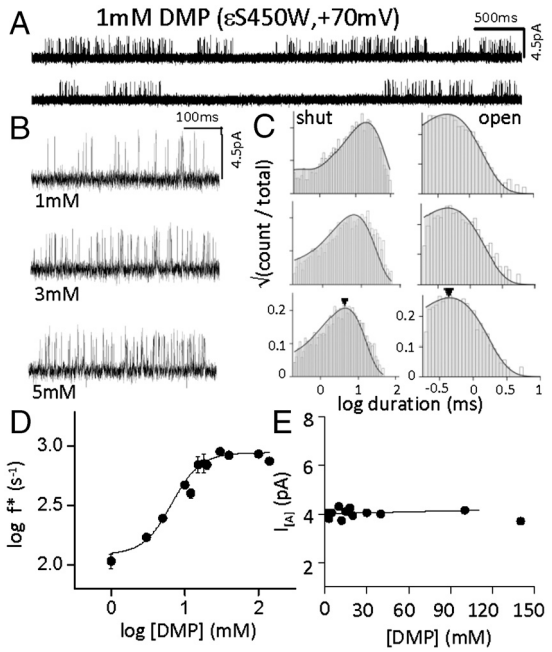

Fig. 3. Gating of εS450W AChRs activated by DMP (+70 mV; construct B1). (*A*) Clusters of openings reflect binding and gating activity of individual AChRs (open is up). (*B*) Higher resolution view of clusters at different [DMP]. (*C*) Intracluster interval duration histograms at different [DMP]. The solid lines are the global fit to Scheme 1 ($K_d = 2.1$ mM, $E_2 = 0.38$). Arrows mark the time constants of the intervals at 5 mM DMP, reference condition (Fig. 2*C*). (*D*) The effective opening rate reaches a plateau at approximately 30 mM ($f_2 = 818$ s^{-1}). (*E*) Depolarization removes channel block so the single-channel current amplitude ($I_{[A]}$) is constant ≤100 mM DMP.

tely eliminated at +70 mV. However, there is no effect of this small degree of block on detection of currents or the f_2 estimate. b_2 was calculated from currents at 100 mM DMP, where no block was apparent. We consider the gating parameters with the B1 background to be the same as for the reference condition (Table 1).

We also measured K_d for DMP (background B1) by fitting intracluster interval durations across different concentrations (Fig. 3*C*): $K_d^{\mathrm{DMP,+70\,mV}} = 2.1$ mM. We fitted the corresponding shut interval durations under the reference condition constraining E_2^{DMP} to be 0.38 (from B1) with the result: $K_d^{\mathrm{DMP,ref}} = 1.9$ mM (Fig. 2*C*). This indicates that K_d is neither voltage-dependent nor affected by the εS450W mutation. We estimate that under the reference condition, K_B/K_d for DMP is approximately 2.3.

We carried out similar analyses for two other AChR agonists, DMT and DMThM. When comparing agonists, we made the assumption that the effect of the B1 background on gating was the same regardless of the activating ligand. This is the same assumption everyone makes for wild-type (WT) receptors when they compare dose-response curves for different agonists. The results for DMT and DMThM are shown in Figs. S3 and S4 respectively, and Table 1. Below, these gating parameters are used to calibrate the effects of mutations.

Table 1. AChR gating parameters

Ligand	f_2(s^{-1})	b_2(s^{-1})	E_2	λ	ΔΔG
ACh	65850	2595	25.4	6251	−5.2
CCh	8603	1612	5.33	2865	−4.7
TMA	5233	2057	2.54	1977	−4.5
DMThM	1561	1630	0.96	1215	−4.2
DMT	1219	2068	0.58	903	−4
DMP	818	2102	0.38	757	−3.9
Cho	101	2181	0.046	267	−3.3

f_2 and b_2 are the diliganded channel-opening and -closing rate constants and E_2 is the diliganded gating equilibrium constant (Fig. S1). λ is the ratio of equilibrium dissociation constants, R vs. R*. The average binding energy difference per agonist molecule, ΔΔG (kcal/mol) $= -0.59\ln(\lambda)$. The parameters are for the B1 background, which is approximately the same as for the reference condition (WT, $\alpha_2\beta\delta\epsilon$, −100 mV, 23 °C).

Using Mutations to Study a Low-Efficacy Agonist. In the next set of experiments, we mutated the AChR to study agonists that support gating rate constants that are too slow to permit convenient analysis under either the reference or block-inhibited condition. Our approach was to add a mutation to B1 that increased E_2 to a small extent. We used the emergent rate constants for DMP, DMT, and DMThM to calibrate the effects of the added mutation on gating.

The added mutation was at position αD97. This loop 5 (loop A) residue is not far from the transmitter binding site but mutations here do not alter K_d^{ACh} or λ^{ACh} and appear to change E_2 exclusively by a parallel change in E_0 (8, 15). Hence, this amino acid does not interact energetically with the agonist or with residues immediately at the binding site that govern affinity. We call the combination (αD97N, εS450W, +100 mV) background B2 (Fig. S2 and Table S2).

With DMP as the agonist, relative to B1 the mutation αD97N increased E_2 by 1.7-fold. We observed approximately the same quantitative effect of this mutation using DMT or DMThM (Fig. 4 and Table S3). This observation shows that the effect of the mutation on gating was the same for these agonists. Considering all three, the fold-increase in E_2 caused by this mutation was 1.67 ± 0.02 (mean ± s.e.). Mutant cycle analyses showed that the εS450W mutation, membrane depolarization, the agonist and the αD97N mutation all act approximately independently to modify the AChR gating rate and equilibrium constants (Table S2).

Choline (Cho) is present at synapses and is a partial agonist of neuromuscular AChRs. Estimates for f_2^{Cho} under the reference conditions range from approximately 90 s^{-1} (16) to approximately 250 s^{-1} (17). Rate constants were measured at both 100 and 140 mM Cho, to be sure that the binding sites were fully-saturated (Fig. S4). Using the average fold-changes in the gating rate constants caused by the αD97N mutant relative to B1 (Table S3) we calculated those for Cho-activated AChRs under the reference condition: $f_2^{\mathrm{Cho,ref}} = f_2^{\mathrm{Cho},B2} * (f_2^{\mathrm{DMP},B2}/f_2^{\mathrm{DMP},B1})$. The results were $f_2^{\mathrm{Cho,ref}} = 101$ s^{-1}, $b_2^{\mathrm{Cho,ref}} = 2181$ s^{-1}, and $E_2^{\mathrm{Cho,ref}} = 0.046$ (Table 1).

Using Mutations to Study High-Efficacy Agonists. The above approach was also used to examine agonists that have faster channel-opening rate constants. Tetramethlyammonium (TMA) and carbamylcholine (CCh) are partial agonists whose gating constants have been estimated previously at the reference condition (18, 19). To estimate the gating parameters for these ligands, we

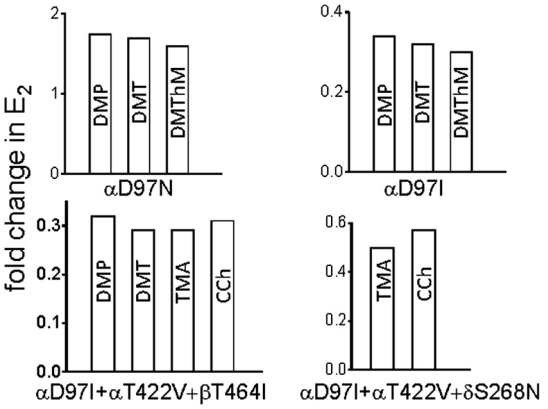

Fig. 4. The effect of background mutations is similar for different agonists. In each plot the fold-change in the gating equilibrium constant E_2 caused by the mutation is given relative to the the B1 background (Table 1 and Table S2).

slowed f_2 by adding the mutation αD97I to B1 (=background B3). This side chain substitution decreases (rather than increases) E_2 (Table S3). First, we assayed the effect of the mutation by using our three "calibrating" agonists. Fig. 4 shows that the effect of this background was to reduce E_2 by approximately the same extent for DMP, DMT, and DMThM (Table S3).

Fig. S4 shows single-channel currents at saturating concentrations for TMA and CCh using B3. After correcting for the effect of the αD97I mutation on each of the observed rate constants, we estimated gating parameters under the reference condition (Table 1). The results are in agreement with those measured directly.

The next agonist we examined was ACh. The $R \rightarrow R*$ channel-opening rate constant (f_2) for this ligand is very fast (41,000 s^{-1} to 85,000 s^{-1}) (16, 19–21) and beyond our ability to measure accurately at the reference condition. The reduction in f_2 caused by the αD97I mutation alone is insufficient to allow the measurement of the gating parameters for ACh, so we added more background mutations to further reduce f_2 and E_2. Because ACh is the natural transmitter we used several different combinations of background and agonist in order increase the accuracy of the gating rate and equilibrium constant estimates (Table 1).

The two background mutations added to B3 were αT422V plus either βT464I or δS268N (B4 and B5). All three of these residues are in the transmembrane domain of the AChR and far from both the transmitter binding sites and αD97 (Fig. S2). Mutant cycle analyses show that voltage, agonists and these mutations have effects on AChR gating that are nearly independent of each other (Table S2, Table S3; Fig. S5). In B4, the fold-changes in f_2, b_2 and E_2 were similar with TMA, CCh, DMP, or DMT as the activating agonist (Fig. 4 and Table S3). In B5 the fold-changes were the same with TMA or CCh. Hence, each of these ligand-background combinations can be used to estimate the reference activation parameters for ACh.

We measured the ACh rate and equilibrium constants with B4 or B5 and used the above fold-changes (relative to B3) for each calibrating ligand to calculate the gating parameters for ACh under the reference condition. There was a close agreement between the estimates obtained with the 6 different agonist/background combinations (Table S4). Taking the average for all calibrations we estimate that ${f_2}^{\mathrm{ACh,ref}} = 65{,}850\ s^{-1}$, ${b_2}^{\mathrm{ACh,ref}} = 2595\ s^{-1}$, and ${E_2}^{\mathrm{ACh,ref}} = 25.4$ (Table 1).

We also estimated K_d for the transmitter using the B4 background. Fitting across concentrations we estimate $K_d^{\mathrm{ACh}} \approx$ 166 μM (Fig. 5*C*), which is similar to the estimate under reference condition (143 μM) (15).

Using Mutations to Study Mutant AChRs. The above, stepwise engineering approach can also be used to study AChRs having mutations that either increase or decrease E_2 substantially. This is important because many interesting mutations increase or decrease the gating rate constants to extents that put these outside the window for analysis under the reference condition and with ACh as the agonist.

We examined two mutations of αP272 (Fig. S6). This amino acid is in the M2-M3 linker of the α subunit, at the interface between the extracellular and transmembrane domains (Fig. 1 and Fig. S2). We chose this residue because reports of the effects of mutations here disagree markedly (22, 23). If the effect of the αP272A mutation is independent of the agonist, then using the values we found with Cho at −100 mV we expect ${f_2}^{\mathrm{DMP}} = 16{,}600\ s^{-1}$, ${b_2}^{\mathrm{DMP}} = 180\ s^{-1}$ and ${E_2}^{\mathrm{DMP}} = 90$. These values are close to the limits of our measurement capabilities so we decided to add a background mutation and use a saturating [DMP], +100 mV to remove channel block. These perturbations together should bring the overall gating rate constants in a more-suitable range for detection and analysis.

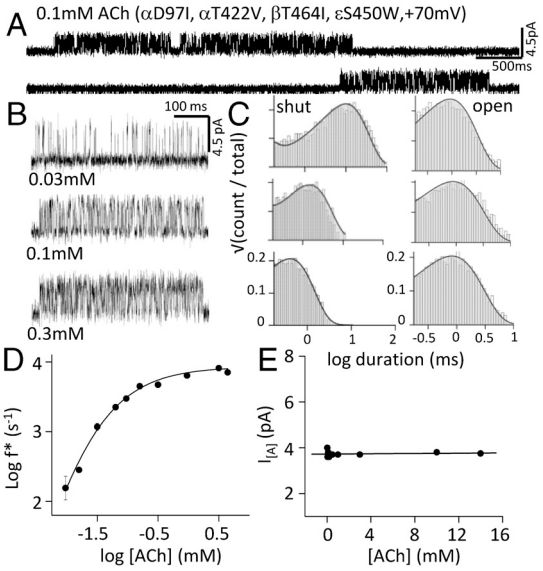

Fig. 5. Gating of AChRs activated by ACh (+70 mV; B4 background). (*A*) Clusters of openings reflect binding and gating activity of individual AChRs (open is up). (*B*) Higher resolution view of clusters at different [ACh]. (*C*) Intracluster interval durations; solid lines are the global fit to Scheme S1 (K_d = 166 μM). (*D*) The effective opening rate reaches a plateau at approximately 1 mM. (*E*) The single-channel current amplitude ($I_{[A]}$) is constant because there is no channel block.

From our database of mutations we chose to add δI43H. In the reference condition this is a high-Φ, loss-of function mutation (reduces ${E_2}^{\mathrm{ACh}}$ by 14-fold, $\Phi = 0.86$) (24). First, we confirmed this effect using another agonist (CCh) and the B1 background. We observed a 12.6-fold decrease in ${E_2}^{\mathrm{CCh}}$, which agrees with the reduction observed using ACh and the reference condition. δI43H is thus calibrated (has effects that are independent of agonist and voltage) and can be used as a tool to study αP272A.

We calculated the combined effect of the background perturbations assuming energy independence (Table S5): ${f_2}^{\mathrm{DMP}} = 818\ s^{-1} * (20.3 * 0.11 * 0.67) = 1277\ s^{-1}$, ${b_2}^{\mathrm{DMP}} = 2102\ s^{-1} * (1.42 * 8.3 * 0.086) = 2130\ s^{-1}$ and ${E_2}^{\mathrm{DMP}} = 0.38 * (238 * 0.079 * 0.08) = 0.57$. The numbers in the parentheses are the fold-increases relative to the reference condition caused by the individual perturbations αP272A (Cho, ref. 23), δI43H and depolarization, respectively. We then measured gating in the {DMP, αP272A,δI43H, + 100 mV} construct and found $f_2 = 1180\ s^{-1}$, $b_2 = 2000\ s^{-1}$ and $E_2 = 0.58$ (Fig. S6). The close agreement between the calculated and observed constants demonstrates both the accuracy of the estimate for αP272A using Cho and the independent nature of the perturbations with regard to both the ground and transition states. Translating back to the reference condition, we estimate that the gating parameters with just the αP272A mutation are: ${f_2}^{\mathrm{ACh}} = 1.2 * 10^6\ s^{-1}$, ${b_2}^{\mathrm{ACh}} = 190\ s^{-1}$ and ${E_2}^{\mathrm{ACh}} = 6{,}326$. This f_2 value is far outside the range of detection and analysis of patch-clamp electrophysiology.

It was reported that αP272A and its neighbor αV46A are energetically coupled ($\Delta\Delta G^{\mathrm{cpl}} = -2.6$ kcal/mol) in the gating reaction (22). We can recalculate the degree of energy coupling between these two residues using the relationship $\Delta\Delta G^{\mathrm{cpl}} = -0.59 \ln[({E_2}^{\mathrm{dbl}} {E_2}^{\mathrm{wt}})/({E_2}^{\alpha\mathrm{P272A}} {E_2}^{\alpha\mathrm{V46A}})]$. With the above, calculated value ${E_2}^{\alpha\mathrm{P272A}} = 6326$, and from experimentally obtained ones that are within the detection window (${E_2}^{\alpha\mathrm{V46A}} = 0.057$ and ${E_2}^{\mathrm{dbl}} = 16$), we estimate that these two mutations essentially do not interact energetically ($\Delta\Delta G^{\mathrm{cpl}} = -0.1$ kcal/mol) in the gating isomerization.

We also examined αP272G, which at the reference condition reduces ${E_2}^{\mathrm{ACh}}$ by 61-fold with a $\Phi = 0.69$ (23). We studied

this mutation using DMP, +100 mV and an additional gain-of-function mutation, εL269F, in the transmembrane M2 helix of the ε subunit (background B7). The effects of agonist, voltage and the εL269F mutation were independent (Table S2). When the αP272G mutation was added to B7, E_2^{DMP} decreased 50-fold and with a Φ value of 0.74. This is similar to its effects using ACh and the reference condition. This result indicates that the effects of αP272G on gating are approximately independent of those for εL269F.

Discussion

The above results show that it is possible to design and control AChR gating. We used this approach to circumvent the bandwidth limitations of single-channel electrophysiology. No other method would allow an accurate estimation of the opening rate constant for αP272A AChRs activated by ACh. It is useful to tailor conditions to make the protein operate in a suitable range for analysis, and then normalize the observed parameters to a reference condition.

The diliganded gating equilibrium constant E_2 is the product of E_0 and λ^2 (Fig. S1). By definition, ligands have no effect on E_0 but differ only with regard to λ. In our experiments, in all cases the effects of mutations and agonists on E_2 were independent. The mutations did not change λ and the agonists did not change the effects of the mutations on gating. The simplest interpretation is that the mutations we studied changed E_2 only by causing an equivalent change in E_0. In support of this hypothesis, for 23 different mutant combinations where E_0 was measured directly (without agonists), the change in E_2 was approximately the same as in E_0 (8).

This pattern is generally observed in the AChR. We have examined thousands of mutations of hundreds of different residues using either Cho or ACh as the agonist (4). So far, mutations of only a few amino acids, all immediately at a transmitter binding site, show a significant effect (>1 kcal/mol) with regard to λ (9, 10). We hypothesize that for the other mutations, the change in E_2 was approximately the same as in E_0. If most of the AChR mutations we have studied have no effect on λ, then it is likely that most naturally occurring mutations, too, mainly modify only E_0. It appears that in AChRs random mutations tune the "gain" of the gating isomerization (the magnitude of E_0) but rarely tinker with the signal coming from the affinity change for the ligands (the magnitude of λ) (25).

A correlate of this hypothesis is that diseases caused by AChR mutations are pathogenic because the receptors have physiologically inappropriate E_0 values. Dozens of mutations cause congenital myasthenic syndromes (CMS) (26) and some of these have been found experimentally to increase E_0 (27). Mutations that change E_0 will influence both the equilibrium and kinetic properties of the AChR. The midpoint of a dose-response profile is a function of E_2 and K_d. A mutation that reduces E_0 will shift the midpoint to a higher agonist concentration and one that increases E_0 will shift it to a lower concentration and might allow a weak agonist (like Cho) to generate a significant and inappropriate leak current. The time constant of the neuromuscular synaptic current (τ) is set, in part, by f_2 and b_2. A mutation that reduces E_0 will decrease τ and one that increases E_0 will increase τ, to an extent that depends on the Φ-value of the mutation. Some CMS mutations are pathogenic because they change E_0 and therefore the dose-response and kinetic properties of neuromuscular AChRs.

The design and control of AChR gating was possible for several reasons. First, all of the various perturbations we examined had effects on gating that are approximately independent of each other (Table S2). These perturbations include mutations, agonists and voltage. Previously we found that 34 of 36 different perturbations show <1 kcal/mol energy coupling and therefore are largely independent with regard to their effect on E_0 (see citations in ref. 28). Even αV46A and αP272A, whose Cα atoms are separated by only 5 Å in the *Torpedo* AChR structure (29), show essentially no energetic interaction. The 15 measurements shown in Table S2 reveal there is some interaction between separated residues, but we found no evidence for long-distance transfer of significant amounts of energy arising from AChR mutations.

The lack of influence of most mutations on λ is further evidence that in the AChR there is little transfer of energy between the transmitter binding sites and distant mutations. Ligands and most side chain substitutions can be considered to be nearly independent perturbations of the relative energy between the R and R* ground states. Such independence of action means that the effects of voltage, mutations and agonists are approximately additive (in terms of energy) with regard to both the gating rate and equilibrium constants. Hence, it was possible to forecast the kinetic behavior of the protein under a multiply perturbed condition simply by multiplying the fold-changes in f_2 and b_2 for each separate perturbation. Without the ability to predict the energies of both the transition and end states it would be much more difficult to engineer AChR gating.

Second, the design of AChRs having arbitrary yet predictable gating properties was greatly facilitated by having a large database of mutations, each with known effects on f_2 and b_2. These became elements of the toolkit we used to control gating. By combining these perturbations it is possible to make AChRs that have an enormous range of rate and equilibrium constants, and, hence, dose-response and kinetic properties.

A third reason why AChR engineering was possible is because this protein's gating isomerization is robust. The ground state structural ensembles (R and R*) and the conformational pathway connecting them are approximately the same with or without ligands at the binding sites, and the energetic consequences of mutations are the same over a >40 million-fold range in equilibrium constant (8). When we compare the same basic fold of the bacterial pentameric ligand gated ion channel (30, 31) and the vertebrate AChR (29) we speculate, reasonably, that these two similarly shaped membrane proteins gate by similar mechanisms even though they have <20% sequence homology. The robustness of pentameric ion channel gating is such that the approximately 2000 mutations separating these distant relatives likely allows for approximately the same mechanism for allosteric conformational change. In AChRs, the combination of the WT sequence, the natural transmitter and −100 mV has been optimized for the physiology of the organism, but there is nothing particularly special about this combination with regard to the physical chemistry of the gating isomerization.

The largely independent effects of mutations on gating implies that energy changes associated with long-range, rigid body and normal mode "breathing" motions are nearly independent of those caused by side chain substitutions. A tilt of the M2 helix (31) and a quaternary twist of the whole protein (32) are structural perturbations that may be correlated with $R \leftrightarrow R*$ energy change. However, these nonlocal structural (energy) changes appear to be mostly independent of local ones caused by mutations and ligands. Conversely, the energy changes caused by mutations and ligands appear not to modify significantly the large scale movements of the protein. It appears that the enthalpy and entropy changes caused by mutations are mainly dissipated locally, close to the amino acid in question.

The gating parameters for four of the seven agonists we studied were previously studied under the reference condition. Our estimates, obtained by using stepwise engineering, are in excellent agreement (Table 1). Our method requires estimating rate/equilibrium constants from multiple backgrounds, so errors in each measurement propagate into the final result. For example, the error in the E_2^{DMP} estimate and that in the effect of the αD97N mutation propagate and create a greater error in the final estimate of E_2^{Cho}. The error value for each perturbation will decrease as alternative backgrounds are employed, because the error associated with each background is independent. The errors

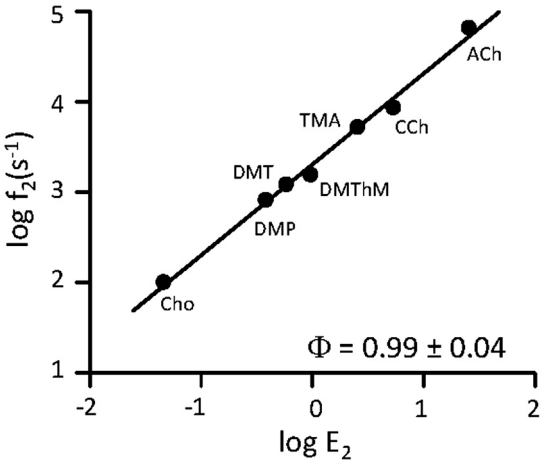

Fig. 6. Rate–equilibrium (R–E) analysis of agonists. The opening rate constant (f_2) is plotted vs. the gating equilibrium constant (E_2) on a log-log scale. The parameters (Table 1) pertain to the B1 and reference conditions (WT AChRs, approximately −100 mV, 23 °C). The slope of the linear fit (Φ) is approximately 1.

on the rate constants estimated by using the engineering approach therefore can be made arbitrarily small.

The gating parameters for the different agonists are plotted in the form of a rate–equilibrium (R–E) relationship in Fig. 6. The slope of this line (Φ) may be an indication of the relative timing of the energy change of the ligand during the gating process, on a scale from 1 (early) to 0 (late) (33). Considering all of the agonists, $\Phi^{\text{agonist}} = 0.99 \pm 0.04$ ($r^2 = 0.991$), which is somewhat higher than previously estimated (0.93) (13).

The agonist coupling constants can be put on an absolute energy scale by using the reference condition value $E_0 = 6.5 * 10^{-7}$ (34). We estimate that on average, each ACh molecule provides −5.2 kcal/mol (−21.8 kJ/mol) toward the gating isomerization and each Cho molecule only −3.3 kcal/mol (−16.3 kJ/mol). This energy is the measure of efficacy and is the metric that should be used to characterize agonists. With protein engineering methods it should be possible to examine a wider array of agonists and AChRs with mutations of binding site residues to gain a deeper understanding of the molecular forces that action shape change in this allosteric protein.

Methods

Mutagenesis and Expression. The mutated residues are shown in Fig. 1. Mutant cDNAs of mouse AChR α, β, δ and ϵ subunits were made using QuickChange Site-directed Mutagenesis Kit (Stratagene) and verified by dideoxy sequencing. HEK 293 cells were transiently transfected using calcium phosphate precipitation. To each 35-mm culture dish of cells approximately 3.5 μg subunit DNA was added in the ratio 2:1:1:1 (α:β:δ:ε) along with cDNA (0.1 μg/μL) encoding green fluorescent protein as a transfection marker. Cells were incubated for approximately 16 h at 37 °C and were then washed with fresh media. Electrophysiological recordings commenced approximately 24 h posttransfection.

Electrophysiology. Single-channel recordings were performed in the cell-attached patch configuration at 23 °C. The bath solution contained either PBS (see below) or (in mM): 142 KCl, 5.4 NaCl, 1.8 $CaCl_2$, 1.7 $MgCl_2$, and 1 Hepes. The pipette solution contained the specified concentration of agonist dissolved in Dulbecco's phosphate buffered saline (PBS; in mM): 137 NaCl, 0.9 $CaCl_2$, 2.7 KCl, 1.5 KH_2PO_4, 0.5 $MgCl_2$, and 8.1 $NaHPO_4$ (pH 7.4). Unless indicated otherwise, the pipette potential was held at −70 mV. Single-channel recording and analyses methods are discussed further in *SI Text*.

Chemical Syntheses. The agonists are shown in Fig. 1. Those that were not available commercially were quaternized from their secondary or tertiary amine precursors using methyl tosylate (*SI Text*). With DMP, we exchanged the tosylate ion for chloride and found no effect of the counter ion on gating.

ACKNOWLEDGMENTS. We thank M. Merritt, M. Shero, M. Teeling, J. Jordan, and C. Nicolai for technical assistance. This work was funded by the National Institutes of Health (NS 064969 and 23513).

1. Edelstein SJ, Changeux JP (1998) Allosteric transitions of the acetylcholine receptor. *Adv Protein Chem* 51:121–184.
2. Sine SM, Engel AG (2006) Recent advances in Cys-loop receptor structure and function. *Nature* 440:448–455.
3. Dougherty DA (2008) Cys-loop neuroreceptors: Structure to the rescue? *Chem Rev* 108:1642–1653.
4. Auerbach A (2010) The gating isomerization of neuromuscular acetylcholine receptors. *J Physiol* 588:573–586.
5. Monod J, Wyman J, Changeux JP (1965) On the nature of allosteric transitions: A plausible model. *J Mol Biol* 12:88–118.
6. Jackson MB (2006) *Molecular and Cellular Biophysics* (Cambridge University Press, Cambridge, UK).
7. Karlin A (1967) On the application of "a plausible model" of allosteric proteins to the receptor for acetylcholine. *J Theor Biol* 16:306–320.
8. Purohit P, Auerbach A (2009) Unliganded gating of acetylcholine receptor channels. *Proc Natl Acad Sci USA* 106:115–120.
9. Purohit P, Auerbach A (2010) Energetics of gating at the apo-acetylcholine receptor transmitter binding site. *J Gen Physiol* 135:321–331.
10. Purohit P, Auerbach A (2010) Glycine hinges with opposing roles at the acetylcholine receptor-channel transmitter binding site. *Mol Pharmacol* 79:351–359.
11. Hille B (1992) *Ion Channels of Excitable Membranes* (Sinauer Associates Inc, Sunderland, MA), 2nd Ed.
12. Neher E, Steinbach JH (1978) Local anaesthetics transiently block currents through single acetylcholine-receptor channels. *J Physiol* 277:153–176.
13. Grosman C, Zhou M, Auerbach A (2000) Mapping the conformational wave of acetylcholine receptor channel gating. *Nature* 403:773–776.
14. Mitra A, Bailey TD, Auerbach AL (2004) Structural dynamics of the M4 transmembrane segment during acetylcholine receptor gating. *Structure* 12:1909–1918.
15. Chakrapani S, Bailey TD, Auerbach A (2003) The role of loop 5 in acetylcholine receptor channel gating. *J Gen Physiol* 122:521–539.
16. De Rosa MJ, Rayes D, Spitzmaul G, Bouzat C (2002) Nicotinic receptor M3 transmembrane domain: Position 8′ contributes to channel gating. *Mol Pharmacol* 62:406–414.
17. Grosman C, Auerbach A (2000) Asymmetric and independent contribution of the second transmembrane segment 12′ residues to diliganded gating of acetylcholine receptor channels: A single-channel study with choline as the agonist. *J Gen Physiol* 115:637–651.
18. Zhang Y, Chen J, Auerbach A (1995) Activation of recombinant mouse acetylcholine receptors by acetylcholine, carbamylcholine, and tetramethylammonium. *J Physiol* 486:189–206.
19. Akk G (2002) Contributions of the non-alpha subunit residues (loop D) to agonist binding and channel gating in the muscle nicotinic acetylcholine receptor. *J Physiol* 544:695–705.
20. Wang HL, et al. (2000) Fundamental gating mechanism of nicotinic receptor channel revealed by mutation causing a congenital myasthenic syndrome. *J Gen Physiol* 116:449–462.
21. Hatton CJ, Shelley C, Brydson M, Beeson D, Colquhoun D (2003) Properties of the human muscle nicotinic receptor, and of the slow-channel myasthenic syndrome mutant epsilonL221F, inferred from maximum likelihood fits. *J Physiol* 547:729–760.
22. Lee WY, Free CR, Sine SM (2008) Nicotinic receptor interloop proline anchors beta1-beta2 and Cys loops in coupling agonist binding to channel gating. *J Gen Physiol* 132:265–278.
23. Jha A, Cadugan DJ, Purohit P, Auerbach A (2007) Acetylcholine receptor gating at extracellular transmembrane domain interface: the cys-loop and M2-M3 linker. *J Gen Physiol* 130:547–558.
24. Purohit P, Auerbach A (2007) Acetylcholine receptor gating: movement in the alpha-subunit extracellular domain. *J Gen Physiol* 130:569–579.
25. Galzi JL, Edelstein SJ, Changeux J (1996) The multiple phenotypes of allosteric receptor mutants. *Proc Natl Acad Sci USA* 93:1853–1858.
26. Engel AG, Shen XM, Selcen D, Sine SM (2010) What have we learned from the congenital myasthenic syndromes. *J Mol Neurosci* 40:143–153.
27. Zhou M, Engel AG, Auerbach A (1999) Serum choline activates mutant acetylcholine receptors that cause slow channel congenital myasthenic syndromes. *Proc Natl Acad Sci USA* 96:10466–10471.
28. Gupta S, Auerbach A (2011) Temperature dependence of acetylcholine receptor-channels activated by different agonists. *Biophys J* 100:895–903.
29. Unwin N (2005) Refined structure of the nicotinic acetylcholine receptor at 4A resolution. *J Mol Biol* 346:967–989.
30. Bocquet N, et al. (2009) X-ray structure of a pentameric ligand-gated ion channel in an apparently open conformation. *Nature* 457:111–114.
31. Hilf RJ, Dutzler R (2009) Structure of a potentially open state of a proton-activated pentameric ligand-gated ion channel. *Nature* 457:115–118.
32. Taly A, et al. (2005) Normal mode analysis suggests a quaternary twist model for the nicotinic receptor gating mechanism. *Biophys J* 88:3954–3965.
33. Zhou Y, Pearson JE, Auerbach A (2005) Phi-value analysis of a linear, sequential reaction mechanism: theory and application to ion channel gating. *Biophys J* 89:3680–3685.
34. Jha A, Auerbach A (2010) Acetylcholine receptor channels activated by a single agonist molecule. *Biophys J* 98:1840–1846.